11

Frequency-selective propagation of spin waves in a three-dimensional magnon T-shaped splitter

© A.A. Martyshkin, E.N. Beginin, A.V. Sadovnikov

Saratov National Research State University,
410012 Saratov, Russia
e-mail: aamartyshkin@gmail.com

Received April 30, 2021
Revised April 30, 2021
Accepted April 30, 2021

Using numerical and experimental methods, the mechanism of control of the transmission of a spin-wave signal in a three-dimensional magnon splitter, formed by an orthogonal junction of magnetic strips of yttrium iron garnet, has been investigated. It is shown that by variation the size of the air gap between the spin-waveguide sections, it is possible to control the selection of the signal propagating in the output sections of the structure. From an applied point of view, the results obtained can be used to create an interconnection element in multilevel magnon information processing devices for the formation of multilayer magnon network topologies and miniaturization of computing devices based on the principles of magnonics. Key words: spin waves, magnonics, three-dimensional interconnections, micromagnetic modeling.

Keywords: spin waves, magnonic, micromagnetic simulations, three-dimensional structure.

DOI: 10.21883/TP.2022.13.52231.134-21

Introduction

Mechanisms and methods of spin waves excitation and control in magnetic materials [1,2] are currently actively studied under scientific fields of the condensed matter physics, such as magnonics [3–5]. Use of signal transmission without motion of charges in the form of the elementary quanta of magnetic excitation (magnons) and spin waves (SW) in dielectric magnetic films is a promising alternative to semi-conductor devices, providing ultra-low energy consumption due to lack of energy ohmic dissipation [6–8]. Improvement of the thin films manufacturing process helps to create micro- and nanostructures, incorporation of which into multi-level schemes allows to create the magnon networks (MN) [9,10], operating principle of which is based on interference effects and allows to code the signal using spin wave amplitude and phase [10,11].

The majority of schemes, based on magnon logic, are magnetized in a plane, thus imposing restrictions on signals routing, since the magnon networks are restricted with a single functional level, have a critical signal propagation length and a large device area [12]. Manufacturing of the structures with vertical transport of a spin-wave signal allows to create three-dimensional magnon networks with a large number of functional blocks in less volume. On the way toward increase of functional elements number in MN it is important to study the mechanisms, responsible for SW transport in multi-level topologies of MN based on three-dimensional structures [13,14].

Recently the concept of three-dimensional magnon structure use has been demonstrated in a magnon crystal, made in the form of meander films of CoFeB [15] and yttrium iron garnets (YIG) [16], consisting of ferromagnetic segments, located at the angle of 90° to each other. Such geometry has the advantage over regular magnon crystals, allowing to evade the restrictions related to SW transport and control in flat magnetized films due to anisotropic dispersion and allowing to propagate SW in three dimensions without significant losses in the transition area.

In this study we propose and study the way of implementation of SW interlevel transport between MN parallel layers based on orthogonally connected magnetic microwave waveguides. The proposed functional element of magnon levels connection allows to implement the frequencies selection, that can be used at implementation of the signals processing algorithms. Using numerical and experimental studies the mechanism of spin-wave transport in the system of two lateral magnetic stripes, orthogonally connected, is demonstrated. The effective selection of the spin-wave signal using an air gap variation in the area of waveguide magnetic stripes junction is shown.

1. Structure and numerical study

For studying the mechanisms of spin-wave connection control the micromagnetic simulation was performed in MuMax3 software [17] based on numerical solution of the Landau–Lifshitz–Gilbert equation:

$$\frac{\partial \mathbf{M}}{\partial t} = -\gamma[\mathbf{H}_{\text{eff}} \times \mathbf{M}] + \frac{\alpha}{M_s}\left[\mathbf{M} \times \frac{\partial \mathbf{M}}{\partial t}\right],$$

that describes the precession of the magnetic moment $\mathbf{M}$ in the effective magnetic field $\mathbf{H}_{\text{eff}} = \mathbf{H}_0 + \mathbf{H}_{\text{demag}} + \mathbf{H}_{\text{ex}} + \mathbf{H}_{\text{a}}$, where $\mathbf{H}_0$ is external magnetic field, $\mathbf{H}_{\text{demag}}$ is

demagnetizing field, $\mathbf{H}_{ex}$ is exchange field, $\mathbf{H}_a$ is anisotropy field. At the same time the anisotropy field was assumed equal to $\mathbf{H}_a = 0$, since the equilibrium magnetization vector is directed along the symmetry axes of YIG [111]. To reduce the signal reflections from the calculated area boundaries the regions with geometrically increasing decay coefficient $\alpha = 10^{-5}-1$ at the waveguide structure boundaries were introduced [18]. For the structure creation the thin YIG films [$Y_3Fe_2(FeO_4)_3$ (111)] with thickness of $10\,\mu$m and saturation magnetization of $4\pi Ms = 1750$ G were used as the magnetic microwaveguides. Dimensionless dissipation parameter was equal to $\alpha = 10^{-5}$, while the exchange hardness – $A_{ex} = 3 \cdot 10^{-7}$ erg/cm. The studied structure can be presented as T-shaped waveguide system in the form of two magnetic stripes that form three spin-wave channels with a length of $S_1 = S_2 = S_2 = 1280\,\mu$m, located in the external homogeneous magnetic field $\mathbf{H}_0 = 370$ Oe, directed along the y axis (Fig. 1, *a*). Magnetization pattern $\mathbf{H}_{int} = \mathbf{H}_0 + \mathbf{H}_{demag}$, observed from the solution of the static problem in waveguide cross sections $S_{1,3}$ and S_2, is presented in Fig. 1, *b* and *c*, respectively. It can be observed that the field $\mathbf{H}_{int}$ almost coincides with $\mathbf{H}_0$ in terms of value, providing the effective excitation of the surface magnetostatic spin waves (MSSW) in the whole structure.

The calculation of the spectral density of the output signal power in the areas, indicated with microstrip antennas ($P_{1,2,3}$) in Fig. 1, was performed. At the same time the input signal of the variable magnetic field, generated by microstrip with current, was set as $b_z(t) = b_0 \sin c(2\pi f_c t)$, where $f_c = 10$ GHz, $b_0 = 10$ mOe. Values of the dynamic magnetization $m_z(x, y, t)$ were recorded with a step $\delta t = 75$ fs within $T = 300$ ns. Then, using Fourier conversion, the frequency dependencies of the dynamic magnetization $P_2(f)$, $P_3(f)$ for the air gap widths $d = 0$, 10, 50, 200 μm at excitation of the spin-wave signal in the port P_1 were built (Fig. 2). Signal detection in the area of port P_2 demonstrates the MSSW spectrum with notches related to the spin-wave signal rotation in the junction area of section S_2 (Fig. 2, *a*). Reduction of the air gap between the sections increases the amplitude of the signal, detected in port P_2. The signal, received in port P_3, corresponds with MSSW spectrum with distortions related to SW decay.

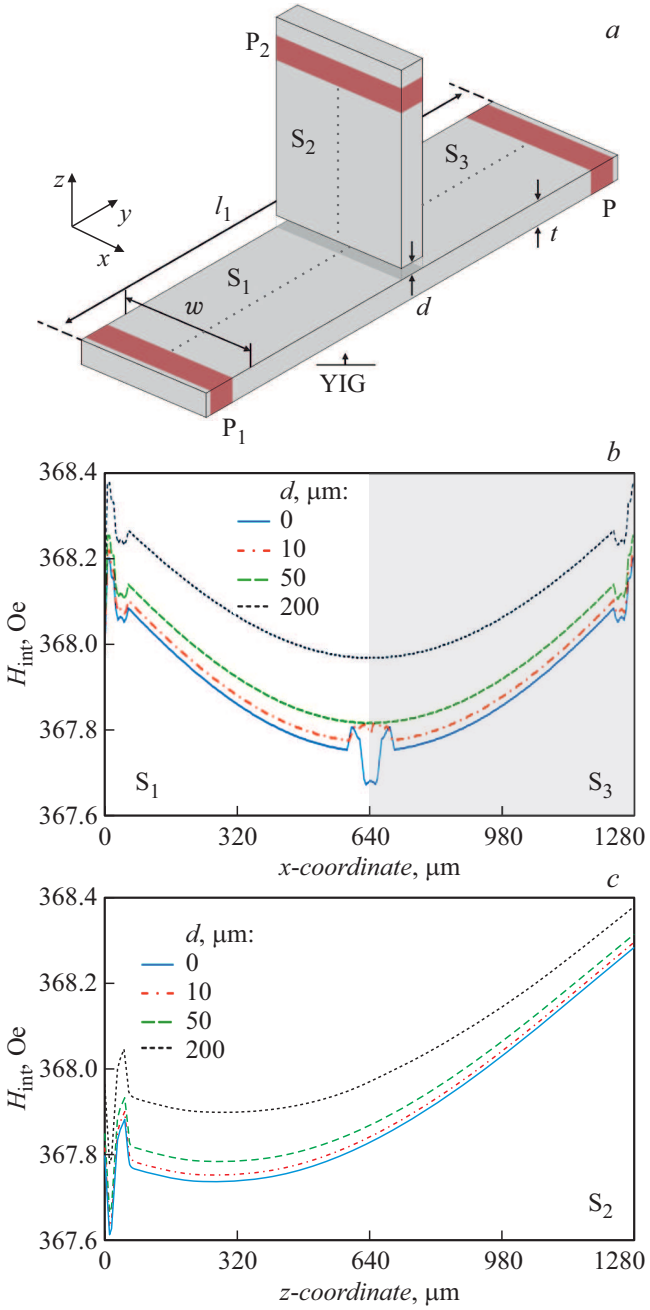

Figure 1. Schematic image of the studied structure (*a*). Distribution of internal magnetic field H_{int} in the structure with a gap in the junction area $d = 0$, 10, 20, 50, 200 μm (*b*) in the central cross section of the waveguide $S_{1,3}$, (*c*) in the central cross section of the waveguide S_2.

2. Experimental study

Using the microwave spectroscopy method, the experimental study of the spin-wave transport in the formed structure by means of microstrip transmission line use was performed. Using laser scribing method, the magnetic strips with width of $w = 500\,\mu$m and thickness of $t = 10\,\mu$m were made from yttrium iron garnet film on a substrate of gadolinium-gallium garnet [(GGG) $Gd_3Ga_5O_{12}$ (111)] with thickness of 500 μm. The length of horizontal sections in the experimental study was $S_1 = S_2 = S_2 = 3000\,\mu$m. SW excitation was performed using the microstrip antenna with thickness of $1\,\mu$m and width of $30\,\mu$m. The structure was put into the static magnetic field, $H_0 = 370$ Oe, oriented along x axis for the effective excitation of MSSW.

At the same time, the measurement of S-parameters was performed at vector network analyzer Agilent Technologies

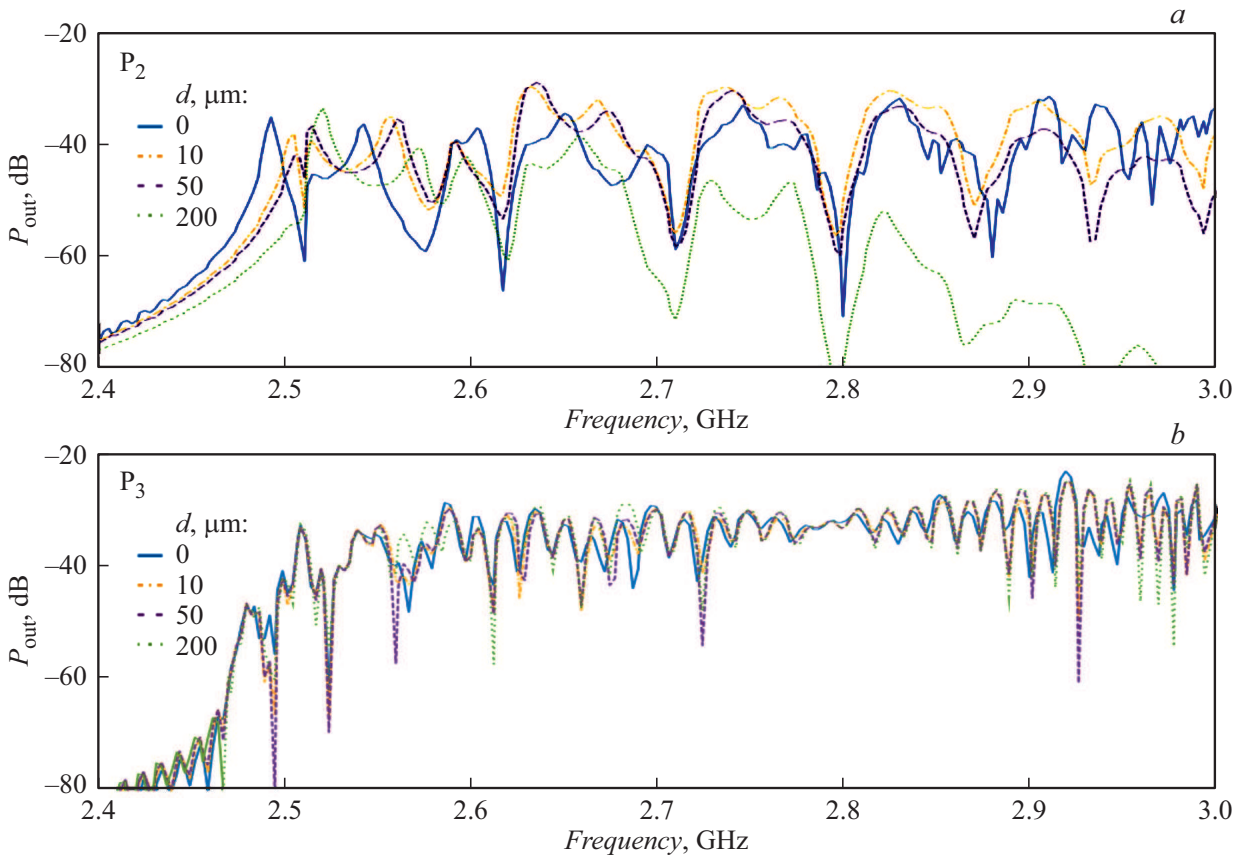

Figure 2. Frequency spectrum of the spin-wave signal, detected in the area (*a*) P_2 and (*b*) P_3 depending on the air gap value.

PNA Network Analyzer E8362C. The measurement results are presented in Fig. 3, where the frequency dependence of parameters S_{nm}, corresponding to signal reception at microstrip transducers P_n $(n = 1, 2, 3)$ at microwave signal excitation on one of the microstrips P_m $(m = 1, 2, 3)$, is shown. In Fig. 3, *a, b* the frequency dependence of module of coefficients S_{31} and S_{13}, corresponding to the signal excitation in port P_1 and P_3 and signal detection in port P_3 and P_1 respectively, is shown. It can be observed that at signal generation in port P_3 the spectral characteristic corresponds with MSSW and the signal is 15 dB higher than at the signal generation in P_1. Such signal drop is related with the signal propagation along the side of magnetic strip, to which the vertical section S_2 is connected. SW signal excitation in ports P_2 and P_1 at detection in ports P_1 and P_2 respectively allows to receive the signal with amplitude of up to −30 dB.

Fig. 3, *c, d* shows the result of the calculation of wave numbers in the range of MSSW excitation frequencies $k = \psi/L$, where ψ is SW phase shift, that happens at length L between input P_n and output P_m in the section. It can be observed that in section S_{13} the excitable wave type (MSSW) results in dependence $f(k)$, that qualitatively corresponds with the dispersion dependence for MSSW mode, shown in Fig. 3, *c* by dashed line D, observed analytically jcite19. However, it can be observed that for S_{31} the phase incursion and effective wave number start to differ from MSSW, which is due the signal propagation along the side of the magnetic strip, to which the vertical section S_2 is connected. Dependence $k_{\text{eff}}(f)$ for case of S_{12} and S_{21} also qualitatively corresponds with the dispersion characteristic of MSSW (Fig. 3, *d*).

Conclusion

Thus, the mechanism of spin-wave signal transmission control in three-dimensional magnon splitter is researched in the work. Using the micromagnetic simulation methods for calculation of equilibrium magnetization pattern the uniform field distribution at orthogonal junction of magnon microwaveguides was shown. Using the numerical calculation of the spin-wave transport characteristics it was demonstrated that in the three-dimensional structure, formed by two magnetic strips, the SW transmission in vertical direction at T-shaped junction is possible, that is confirmed with the experimental results. It was shown, that with variation of the value of air gap between spin-wave sections it is possible to perform the spatial-frequency selection of the signal. In terms of application, the observed data can be used for creation of the elementary

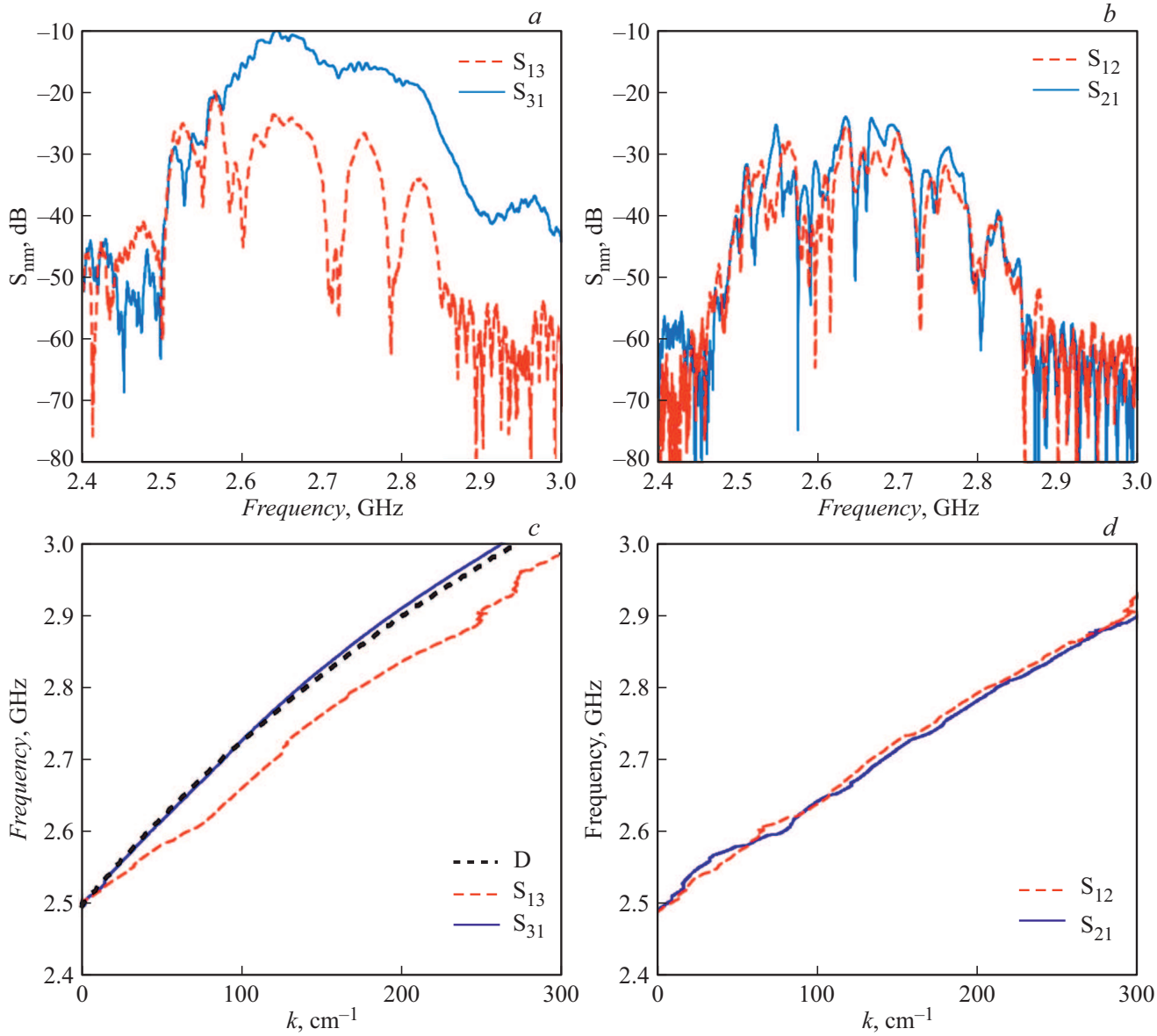

Figure 3. Frequency dependence of module of coefficients S_{nm} in sections $S_{1,3}$ (*a*) and $S_{1,2}$ (*b*). Calculation of effective wave numbers S_{nm} in sections $S_{1,3}$ (*c*) and $S_{1,2}$ (*d*).

interconnection element in multi-layer information processing systems, which use will allow to increase density of arrangement of the three-dimensional magnon network functional elements.

Funding

The study was performed with support of the Ministry of Education and Science of Russia under the Government Task (project №FSRR-2020-0005).

Conflict of interest

The authors declare that they have no conflict of interest.

References

[1] V.V. Kruglyak, S.O. Demokritov, D. Grundler. J. Phys. D, **43**, 264001 (2010).
[2] A.V. Chumak, V.I. Vasyuchka, A.A. Serga, B. Hillebrands. Nature Phys., **11**, 453 (2015).
[3] K. Roy, S. Bandyopadhyay, J. Atulasimha. Appl. Phys. Lett., **99**, 063108 (2011).
[4] Yi-Pu. Wang, J.W. Rao, Y. Yang, Peng-Chao Xu, Y.S. Gui, B.M. Yao, J.Q. You, C.-M. Hu. Phys. Rev. Lett., **123**, 127202 (2019).
[5] A.V. Sadovnikov, E.N. Beginin, S.E. Sheshukova, Yu.P. Sharaevskii, A.I. Stognij, N.N. Novitski, V.K. Sakharov, Yu.V. Khivintsev, S.A. Nikitov. Phys. Rev. B, **99**, 054424 (2019).
[6] S. Neusser, D. Grundler. Adv. Mater., **21**, 2927 (2009).

[7] S.A. Nikitov, A.R. Safin, D.V. Kalyabin, A.V. Sadovnikov, E.N. Beginin, M.V. Logunov, M.A. Morozova, S.A. Odintsov, S.A. Osokin, A.Yu. Sharaevskaya, Yu.P. Sharaevsky, A.I. Kirilyuk. Phys. Usp., **63**, 945 (2020).
[8] D. Sander, S.O. Valenzuela, D. Makarov, C.H. Marrows, E.E. Fullerton, P. Fischer, J. McCord, P. Vavassori, S. Mangin, P. Pirro, B. Hillebrands, A.D. Kent, T. Jungwirth, O. Gutfleisch, C.G. Kim, A. Berger. J. Phys. D, **50**, 363001. (2017).
[9] A.V. Sadovnikov, E.N. Beginin, S.E. Sheshukova, D.V. Romanenko, Y.P. Sharaevsky, S.A. Nikitov. Appl. Phys. Lett., **107**, 202405 (2015).
[10] R. Perricone, X.S. Hu, J. Nahas, M. Niemier. Design of 3d nanomagnetic logic circuits: A full-adder case study, Design, Automation & Test in Europe Conference & Exhibition (DATE), 2014 10.7873/date.2014.132 (2014).
[11] A. Khitun, M. Bao, K.L. Wang. J. Phys. D, **43**, 264005 (2010).
[12] M.T. Niemier, G.H. Bernstein, G. Csaba, A. Dingler, X.S. Hu, S. Kurtz, S. Liu, J. Nahas, W. Porod, M. Siddiq, E. Varga. J. Phys.: Condens. Matter., **23**, 493202 (2011).
[13] E. Beginin, A. Sadovnikov, V. Sakharov, A. Stognij, Y. Khivintsev, S. Nikitov. J. Magn. Magn. Mater., **492**, 165647 (2019).
[14] E.N. Beginin, A.V. Sadovnikov, A.Y. Sharaevskaya, A.I. Stognij, S.A. Nikitov. Appl. Phys. Lett., **112**, 122404 (2018).
[15] G. Gubbiotti, A. Sadovnikov, E. Beginin, S. Nikitov, D. Wan, A. Gupta, S. Kundu, G. Talmelli, R. Carpenter, I. Asselberghs, I.P. Radu, C. Adelmann, F. Ciubotaru. Phys. Rev. Appl., **15**, 014061 (2020).
[16] V.K. Sakharov, E.N. Beginin, Y.V. Khivintsev, A.V. Sadovnikov, A.I. Stognij, Y.A. Filimonov, S.A. Nikitov. Appl. Phys. Lett., **117**, 022403 (2020).
[17] A. Vansteenkiste, J. Leliaert, M. Dvornik, M. Helsen, F. Garcia-Sanchez, B. Van Waeyenberge. AIP Adv., **4**, 107133 (2014).
[18] G. Venkat, H. Fangohr. J. Magn. Magn. Mater., **34**, 450 (2018).
[19] R. Damon, J.R. Eshbach. J. Phys. Chem. Solids, **19**, 308 (1961).